MASS TRANSFER IN STRUCTURED PACKING

André B. Erasmus and Izak Nieuwoudt

Institute for Thermal Separation Technology, Department of Chemical Engineering, University of Stellenbosch, South Africa.

ABSTRACT

A short wetted-wall column was used to investigate the gas phase mass transfer of pure organic liquids evaporating into an air stream. No liquid side resistance was observed for the binary systems investigated. Both smooth and textured surfaces were used in the study and the experimental results were correlated with a power law series. The correlations for the different surfaces were tested in two predictive models using distillation experimental data for the three binary test systems under conditions of total reflux. The correlations for the textured surface gave better predictions of the HETP than correlations proposed in literature. The modelling of effective surface area was identified as an area in which more research is needed. A preliminary study showed that the mass transfer coefficients predicted with computational fluid dynamics (CFD) is significantly higher than that predicted by correlations derived from wetted-wall evaporation data.

Keywords: Wetted-wall, correlations, structured packing, effective area, CFD

INTRODUCTION

Several models exist to model the mass transfer process in structured packing [1-6]. In most of these models, effective surface area and mass transfer coefficients were not measured separately. In this study the focus has been put on decoupling these two phenomena by measuring and modelling the gas phase mass transfer under conditions of total wetting. A wetted-wall column was used to measure gas phase mass transfer coefficients and to evaluate liquid side resistances. Both smooth and textured surfaces were used in our experimental study. The results were correlated with a simple power law series. The different correlations were combined with existing hydraulic models and their accuracy determined against experimental distillation data. There is always doubt in calculating the effective surface area in structured packing and most published mass transfer models differ in this regard.

This prompted the use a CFD model to 'measure' the gas phase mass transfer coefficient in structured packing (under conditions of total wetting). CFD has been used in the past as a design tool for structured packing [7]. Advances in computing power has made it possible to use so called 'low Reynolds number turbulence models' [8] and get results in a reasonable time. The commercial CFD package CFX [9] was used in this study. This paper is divided into three parts. The first part briefly presents the wetted-wall experimental results. The second part is focused on experimental distillation results and the final part looks at the CFD model and preliminary results.

MASS TRANSFER IN A WETTED-WALL COLUMN

Gas Phase Mass Transfer

The gas phase mass transfer was studied by evaporating several pure components in a short wetted-wall column [10]. This differs from the work done by previous researchers who used a longer wetted-wall column [11, 12]. The reasoning behind using a shorter column is that in structured packing entrance effects is expected to have a significant effect on the gas phase mass transfer. For a description of the experimental set up and –procedure, the reader is referred to previous papers published in this regard [10, 13, 14]. Only the results will be presented here.

The gas phase mass transfer coefficients were determined for the evaporation of pure components from both a smooth and a textured surface. The experimental set up allowed for isothermal operation. The textured surface used in this study is similar to that of the widely used metal Flexipac range of structured packing from Koch. The experimental results were correlated with the simple, customary power law series with the relevant dimensionless numbers. Table 1 shows the best performing correlations for the smooth surface and Table 2 the correlations for the textured surface. The mass transfer rate was found to be higher from a liquid flowing over a textured surface compared to a liquid flowing over a smooth surface. Correlations containing a relative gas phase Reynolds number perform better than correlations without them. In fitting the correlations the exponent of the gas phase Schmidt number was set equal to the theoretical value of 0.5 [15]. The liquid film thickness was taken into account in calculating the equivalent diameter of the tube:

$$d_{eq} = d - 2\delta \qquad (1)$$

Table 1 Correlations (smooth surface).

Correlation	RMS error*
1. $Sh_g=0.0045Re_gSc_g^{0.5}$	3.206
2. $Sh_g=0.00086Re_{g,r}^{1.17}Sc_g^{0.5}$	2.475

Table 2 Correlations (textured surface).

Correlation	RMS error*
3. $Sh_g=0.04635Re_g^{0.75}Sc_g^{0.5}$	4.445
4. $Sh_g=0.00827Re_{g,r}^{0.94}Sc_g^{0.5}$	3.820

$$* \text{ RMSerror} = \sqrt{\frac{\left(Sh_{\text{experimental}} - Sh_{\text{predicted}}\right)^2}{n}}$$

Liquid Phase Mass Transfer

Liquid phase mass transfer was investigated by evaporating binary mixtures with one or both volatile components. In most cases no liquid side resistance was found for the systems investigated. For systems with both components volatile, the measured overall mass transfer coefficient was the same as the predicted gas phase mass transfer coefficient. For systems with only one volatile component no liquid side resistance was found but rather an enhancement of the gas phase mass transfer rate. This enhancement was thought to be due to surface tension differences between solvent and solute. For more details the reader is referred to [10].

In subsequent sections the gas phase mass transfer correlations in Table 1 and Table 2 will be compared with one another and existing correlations. Where the correlations in tables 1 and 2 were used, liquid phase resistance was ignored.

BINARY DISTILLATION

To test the proposed correlations, and because of a lack of published distillation data, numerous total reflux distillation experiments were performed using different binary systems. The binary systems used in this study were chlorobenzene/ethylbenzene, acetone/methanol and ethanol/isopropanol.

Theory

Predictive models

There are quite a few models published in the open literature to predict structured packing performance [1-6, 16, 17]. The two most widely published models are that of the University of Texas Separations Research Program (SRP model) [18] and the Delft University of Technology (Delft model) [3, 18]. These models have been tested in depth and were found to perform reasonably well.

In the SRP model the structured packing bed is modelled as a series of inclined wetted-wall columns. The packing side dimension (S) is used as the characteristic length parameter in the mass transfer correlations. Packing specific parameters that must be known include dry pressure drop data and pressure drop at the flooding point. The effective surface area is calculated through a modified Shi and Mersmann equation [19] with a surface enhancement factor that must be supplied. The correlation proposed by Johnstone and Pigford [20] for gas phase mass transfer in

wetted-wall columns was first used [21] and modified later [2] to fit experimental distillation data. The penetration model with a modified exposure time is used to calculate the liquid phase mass transfer coefficient.

In the Delft model the vapour phase is assumed to follow a zigzag flow pattern through the packing elements. The characteristic length parameter used in the model is the hydraulic diameter at the crossing of corrugations and is much smaller than that of the SRP model. The pressure loss at the crossing of corrugations is thought to be the main contributor to overall pressure drop, with a much smaller contribution from vapour/liquid friction. A correlation for the effective surface area was fitted on experimental absorption data. The overall gas phase mass transfer coefficient is calculated from laminar and turbulent contributions. The laminar and turbulent contributions are calculated from analogous heat transfer correlations. The expression for the liquid phase mass transfer coefficient is the same as the SRP model, but with their defined hydraulic diameter used as the characteristic length parameter.

Calculating packing height

The height of packing that produces a concentration change that would be produced by an equilibrium stage, commonly referred to as HETP, can be calculated with the HTU/NTU concept [22]. Due to the dominant resistance being in the gas phase for distillation, the calculation is based on the gas phase. The height equivalent to a theoretical plate (HETP) is calculated by multiplying the height of a transfer unit with the number of transfer units in a theoretical plate:

$$\mathrm{HETP} = \mathrm{HTU}_{\mathrm{oG}} \times \mathrm{NTU}_{\mathrm{oG}} \tag{2}$$

If it is assumed that the slope of the equilibrium line and the slope of the operating line are constant over a theoretical stage then the number of transfer units can be approximated with [23]:

$$\mathrm{NTU}_{\mathrm{oG}} = \frac{\ln(\lambda)}{(\lambda - 1)} \tag{3}$$

where

$$\lambda = \frac{\mathrm{G}}{\mathrm{L}}\mathrm{m} \tag{4}$$

By adopting the two-film theory it can be shown that:

$$\mathrm{HTU}_{\mathrm{oG}} = \mathrm{HTU}_{\mathrm{G}} + \lambda \mathrm{HTU}_{\mathrm{L}} \tag{5}$$

where

$$\mathrm{HTU}_{\mathrm{G}} = \frac{u_{\mathrm{Gs}}}{k_{\mathrm{G}} a_{\mathrm{e}}} \tag{6}$$

and

$$HTU_L = \frac{u_{Ls}}{k_L a_e} \quad (7)$$

The total height of packing needed for a separation is the sum of the individual HETP for each equilibrium stage:

$$h_{packing} = \sum_{i=1}^{n} HETP_i \quad (8)$$

An equilibrium stage model was used to calculate the flow, composition, and temperature profiles throughout the column.

Assumptions, Thermodynamics and Transport Properties

Certain assumptions were made before the distillation data could be modelled with the SRP and Delft models.

For the SRP model the dry pressure drop was calculated using a correlation proposed in an earlier article by the same authors [1]. A flooding pressure drop of 11 mbar/m was assumed. A surface enhancement factor (F_{SE}) of 0.35 was used.

In the Delft model the height of a packing element and the height of the packed bed have to be supplied. The height of a packing element must be smaller than the diameter of the column in order to calculate a so called 'directional change loss coefficient'. For the packing used in this study the height of the packing elements (265 mm) was more than the column diameter (200 mm). An element height of 0.199 m was assumed in the model. The packed bed height was calculated using the actual packing element height. The constants published for Montzpak B1-250 [3] was used in the effective surface area correlation.

For all the systems studied the NRTL model was used to calculate the liquid phase activity coefficient. An ideal vapour phase was assumed. For the chlorobenzene/ethylbenzene system vapour/liquid equilibrium data was taken from [24]. The vapour pressure equations used were fitted on the predicted values from the equations in [24] and experimental values from [25]. For the acetone/methanol system measured VLE data was used. In the ethanol/2-propanol case the NRTL parameters in the SIMSCI databank were used after being verified with experimental measurements. For the acetone/methanol and ethanol/2-propanol systems vapour pressure equations from [26] were used.

Table 4 lists the different models used for mixture transport properties. All the models are summarized in [26].

Table 4 Mixture transport properties [26].

Property	Liquid phase	Vapour phase
Viscosity	Grunberg and Nissan	Reichenberg
Diffusion coefficient	Tyn and Callus	Wilke and Lee
Surface tension	Winterberg	N/A

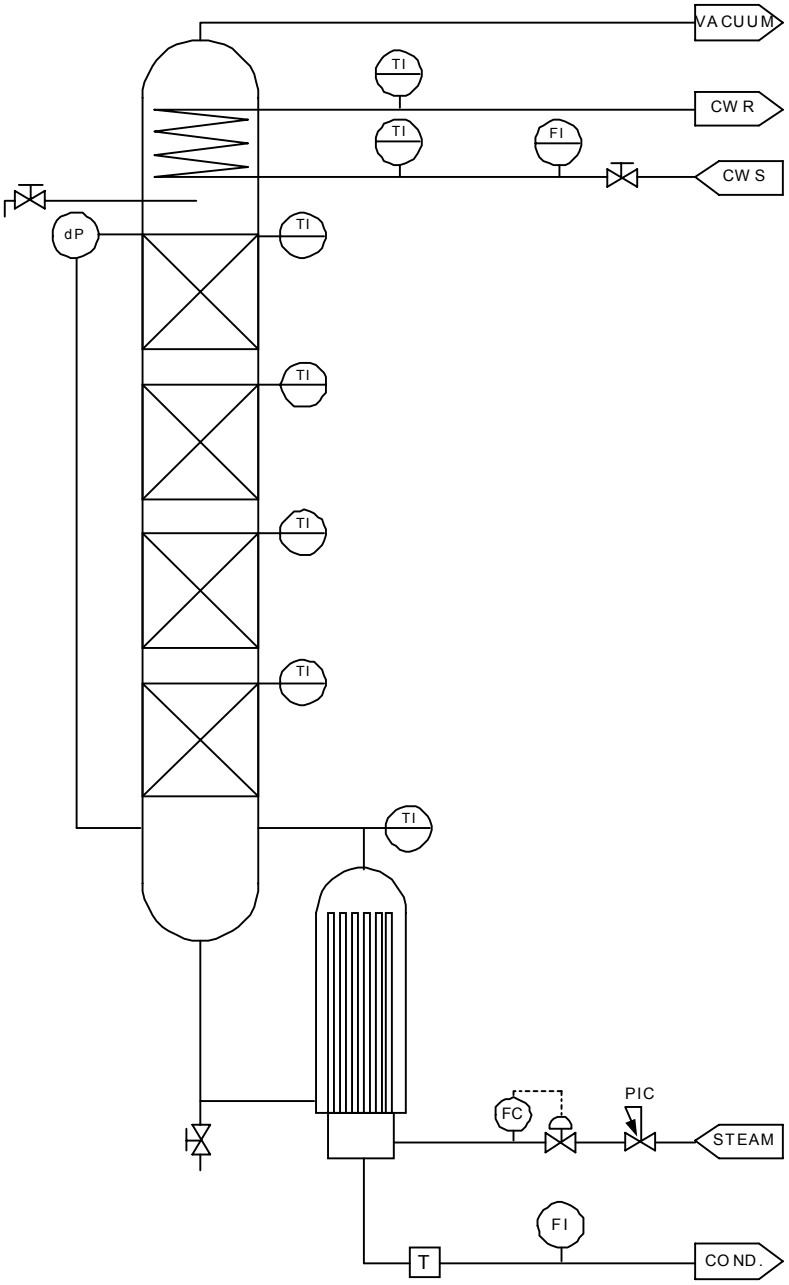

Figure 1 Total reflux distillation column

Experimental Set Up

The column used was specifically set up for experimental work under conditions of total reflux. The condenser was located at the top of the column and all the distillate simply fell back into the top redistribution pan (figure 1). The column was constructed out of 200 mm ID glass segments and varied in height. It had either three or four packed sections. A thermosyphon type reboiler without a baffle in the sump was used. A distillate sample was drawn from the top redistribution pan and a bottoms sample from the sump. In some instances an intermediate sample was drawn between the third and fourth packed sections (chlorobenzene/ethylbenzene system).

Chimney type redistributors were used with a drip point density of 795 m^{-1}. The packed sections were insulated with ceramic wool and polyethylene foam.

The following temperatures were measured:

- Reboiler return temperature
- Temperature below the packing
- Temperature at the top of each packed segment
- Cooling water inlet and outlet of the condenser

The pressure drop over the column as well as the cooling water- and condensate flow rates were also measured.

The low inventory in the reboiler of the column (less than 14 litres) made it possible to reach steady state in a short period of time. After start up the column was left for 3 hours to reach equilibrium before the first samples were drawn. A small change in the heating duty was made and the column was then left for 2-2½ hours before the next samples were drawn. The composition of the samples was determined by means of gas chromatography.

The experimental results are available on request.

Results and Discussion

Figures 2 to 6 show the results for the different test systems. The predicted packing height according to the SRP and Delft models are shown. Included in the figures are the predicted packing heights when the gas phase mass transfer correlations in the SRP and Delft models were substituted with correlations 1 to 4. The results are plotted as a function of the packing load factor (F_G). Table 4 summarizes the results for the different correlations with the different models.

From figures 2 to 6 and table 5 it is evident that the SRP model performs better in predicting the packed height compared to the Delft model. The correlations fitted on the packing wetted-wall data, correlations 3 and 4, seem to fare better in both models compared to the correlations suggested by the authors of these models. In the wetted-wall studies it was found that the microstructure of the packing enhanced the gas phase mass transfer [10], and it should therefore be expected that correlations 3 and 4 perform better than correlations 1 and 2.

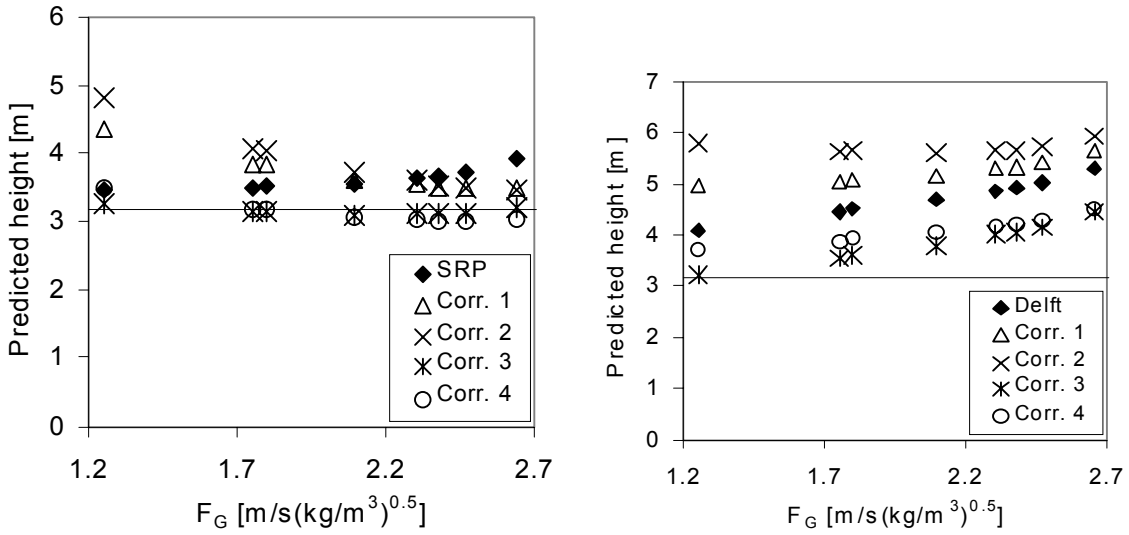

Figure 2 *Results: SRP and Delft models with different correlations for the system chlorobenzene/ethylbenzene, total reflux, 1.01 bar. Actual height (—).*

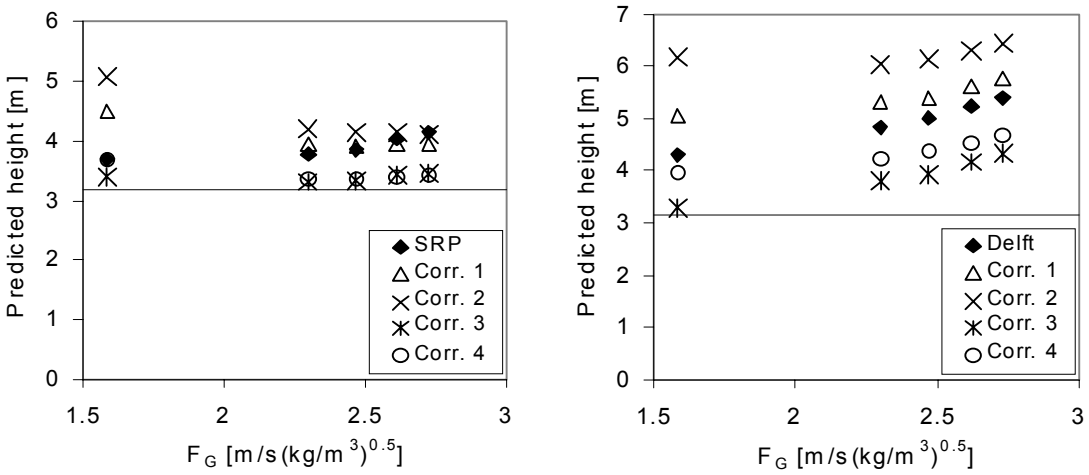

Figure 3 *Results: SRP and Delft models with different correlations for the system chlorobenzene/ethylbenzene, total reflux (0.6 bar A). Actual height (—).*

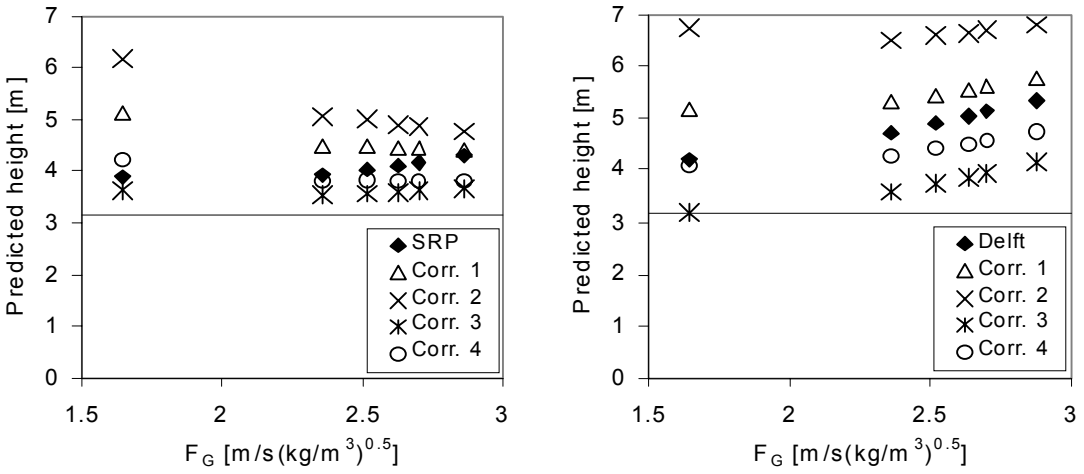

Figure 4 *Results: SRP and Delft models with different correlations for the system chlorobenzene/ethylbenzene, total reflux (0.3 bar A). Actual height (—).*

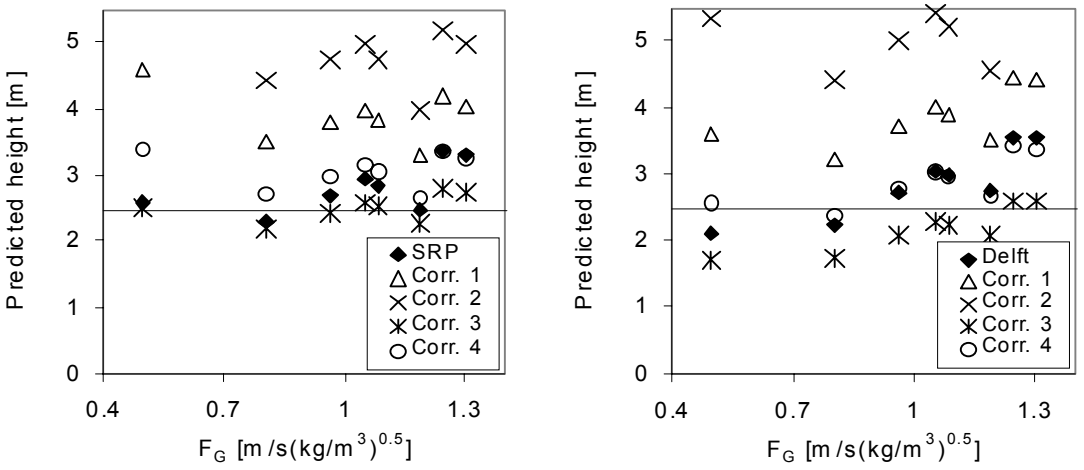

Figure 5 *Results: SRP and Delft models with different correlations for the system acetone/methanol, total reflux (1.01 bar A). Actual height (—).*

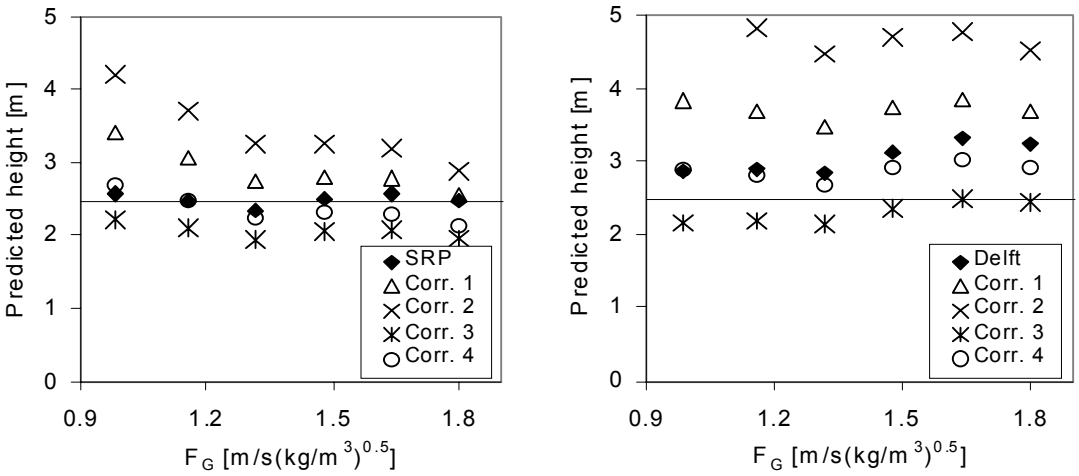

Figure 6 Results: SRP and Delft models with different correlations for the system ethanol/2-propanol, total reflux (1.01 bar A). Actual height (—).

Table 4 Results of different correlations with SRP and Delft models.

Correlation	RMS error*	
	SRP	Delft
SRP	0.584	N/A
Delft	N/A	1.352
correlation 1	1.073	1.888
correlation 2	1.679	2.827
correlation 3	0.288	0.612
correlation 4	0.470	0.915

$$* \text{RMSerror} = \sqrt{\frac{\left(h_{\text{experimental}} - h_{\text{predicted}}\right)^2}{n}}$$

The effective surface area is a point of debate and differs widely in its prediction by the SRP and Delft models. All the data shown in the above figures are for total reflux distillation and under these conditions almost complete wetting should be expected. Figure 7 shows the predicted effective surface area for the chlorobenzene/ethylbenzene test system. The Delft model predicts an almost constant affective surface area, equal to about 90% of the packing area. Even at conditions close to flooding, the SRP model only predicts an affective surface area of 78% of the packing area. Given the good results obtained with the SRP model, it seems that the effective surface area was modelled erroneously and the gas phase mass transfer used as a fitting parameter to fit the overall model to distillation data. In a more recent publication [18] the use of the Onda correlation [27] to calculate effective surface area was proposed. Incorporating this effective surface area into their model would lead to optimistic packed height estimation. The mass transfer correlations would have to be refitted on their distillation data.

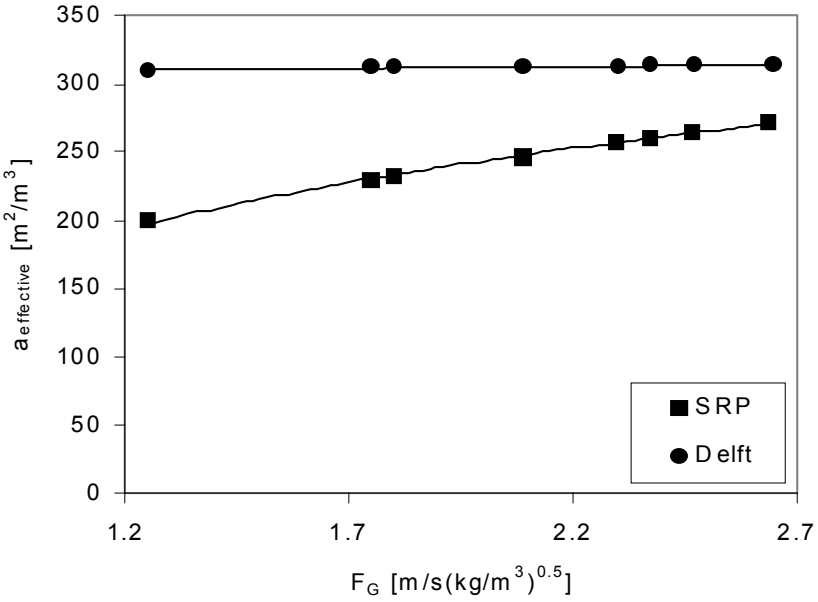

Figure 7 Effective surface area for chlorobenzene/ethylbenzene system, total reflux (1.01 bar A).

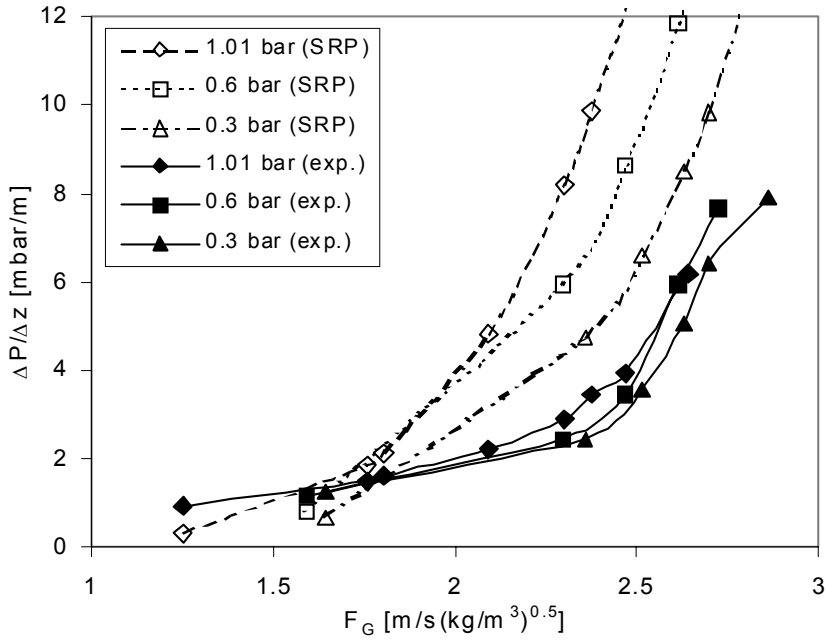

Figure 8 Comparison between measured and predicted pressure drop for the chlorobenzene/ethylbenzene system using the SRP model.

Figure 8 and 9 compare the pressure drop calculated with the SRP and Delft models with the measured values for the chlorobenzene/ethylbenzene system.

The same method is used by both models to predict the loading point [28]. In the SRP model a flooding pressure drop has to be supplied. A flooding pressure drop of

11.0 mbar/m was used for this system. This is slightly higher than the recommended value of 10.25 mbar/m [18], but convergence difficulties were experienced when using the recommended value. Figure 8 shows that the SRP model predicts higher pressure drops for F_G>1.8 compared to experimental measurements. The pressure drop predicted with the Delft model (figure 9) is also higher than the measured values for F_G>1.8, although closer than compared to the SRP model. The measured pressure drop suggests that the loading point of Flexipac 350Y is higher than predicted by the model of Verschoof et.al.[28], at around F_G=2.25.

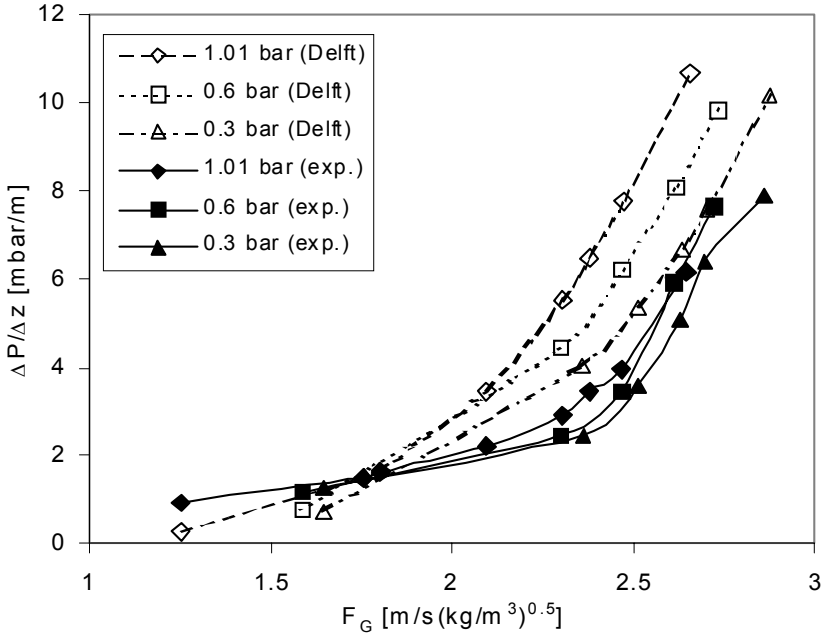

Figure 9 Comparison between measured and predicted pressure drop for the chlorobenzene/ethylbenzene system using the Delft model.

The proposed correlations do perform well when used in the SRP model. The results should however be judged carefully keeping in mind the mentioned uncertainty in the calculation of the effective surface area. In the Delft model the effective surface area is calculated with a correlation fitted on experimental data for the absorption of atmospheric CO_2 in caustic solutions [3, 29]. Aqueous solutions are notoriously non-wetting and their use to predict the hydraulic performance of structured packing has been questioned before [30]. More research is needed in this area, preferably with organic liquids.

Overall both models would lead to a conservative design when using Flexipac 350Y. A major drawback of the SRP model is the number of packing type- and size specific constants, which is difficult to obtain or would be cumbersome to measure. The Delft model contains less packing specific constants. Such constants are however needed to calculate the effective surface area. In order for the SRP and Delft models to be more accurate a better understanding of gas phase mass transfer and effective surface area are required. It would also be easier to incorporate such models into the Delft model.

It is proposed that the gas phase mass transfer be measured and modelled separately in the structured packing, instead of fitting a mass transfer correlation to the experimental data. One possible way is to measure the evaporation rate for pure organic liquids from the packing surface. There will be no liquid phase resistance and by working on a relative small diameter column, and ensuring an even liquid phase distribution, conditions close to total wetting could be attained. Effective surface area measurements should also be made using organic liquids, as mentioned before. Current research by the authors is focussed in these areas. The use of computational fluid dynamics (CFD) to quantitatively predict the gas phase mass transfer is also under investigation. Preliminary results will be presented in the next section.

CFD AND MASS TRANSFER IN STRUCTURED PACKING

Introduction

The exponential growth of computing power and modern CFD codes utilizing efficient algorithms have made CFD a powerful tool in flow analysis. It has been used in the past with some success in the development of new geometries for structured packing [7]. It has also been used more recently in the modelling of radial and axial dispersion in catalytically packed structured packing [31]. Some attempts have also been made at modelling complete columns containing random packing [32].

Mass and heat transfer in cross-corrugated passages is not only limited to structured packing applications. Compact heat exchangers also have a cross-corrugated geometry. The heat transfer in these types of heat exchangers has been modelled using CFD and compared with experimental measurements [33, 34] The idea of using CFD as the basis for a correlation for mass transfer coefficients is not new and has been used in the past to predict mass transfer in sudden pipe expansions at high Schmidt numbers [35, 36] and for corrosion rates in pipe elbows [37].

In recent studies [7] the liquid phase has been ignored and the focus has been on modelling the flow of the vapour phase through the packing elements. The understanding of separated two-phase flows is still in its infancy and a lot of research effort is focused in this area [38-40]. In this research the liquid phase will also be ignored. The gas phase mass transfer of a species from the wall of a smooth tube and a structured packing element will be investigated.

Theory

A detailed description of the elements of a CFD code and turbulence modelling can be found elsewhere [41, 42]. Some remarks concerning turbulence will be given here.

When using a low-Reynolds-number turbulence model the fitting of a wall function is avoided and the boundary layer is resolved. This necessarily leads to fine grids, which in turn requires more computing resources. The advantage is a more accurate approach towards modelling transport processes in close proximity to a wall in turbulent flows. A detailed description of the low-Reynolds-number k-ε model is given in [8].

Different turbulence models were used in the work on compact heat exchangers mentioned before [33]. The low-Reynolds-number k-ε model gave more accurate results when compared to the standard k-ε model. In the present study the low-Reynolds-number k-ε turbulence model was used.

In calculating a mass transfer coefficient the same approach has been followed as discussed in a previous paper [10], i.e. diffusion of a species through a stagnant gas. Mole fractions instead of partial pressures have been used and the final form of the equations are as follows:

$$k_G = \frac{N_A (x_{Bm})_{ave}}{C_T \Delta x_A} \tag{9}$$

A logarithmic average of the inlet and outlet of the molar fraction driving force is used:

$$\Delta x_A = \frac{(x_{Ai} - x_{Ab})_{inlet} - (x_{Ai} - x_{Ab})_{exit}}{\ln\left(\frac{(x_{Ai} - x_{Ab})_{inlet}}{(x_{Ai} - x_{Ab})_{exit}}\right)} \tag{10}$$

An arithmetic average of the logarithmic mean of x_{Bi} and x_{Bb} between the inlet and outlet is used:

$$(x_{Bm})_{ave} = \frac{1}{2}\left((x_{Bm})_{inlet} + (x_{Bm})_{outlet}\right) \tag{11}$$

where

$$x_{Bm} = \frac{x_{Bb} - x_{Bi}}{\ln\left(\frac{x_{Bb}}{x_{Bi}}\right)} \tag{12}$$

Values for the bulk phase molar fraction of the diffusing specie were obtained by calculating the average inlet or outlet concentration of the specie. The interface mole fraction was specified as a wall boundary condition. A simple mass balance between the inlet and outlet determined the flux of the ‘evaporating’ specie.

The equivalent diameter for the packing was calculated as:

$$d_{eq} = \frac{Bh}{S} \qquad (13)$$

The CFD package CFX 4.4 [9] was used. The package solves the Navier Stokes equations on a volume-conserved basis, using body fitted grids, with a non-staggered grid and variables evaluated at cell centres. An improved version of the Rie-Chow algorithm [43] is used with the SIMPLEC [44] algorithm to solve the pressure-velocity coupling.

Model and Results

In order to test the validity the low-Reynolds-number k-ε turbulence model, the wetted-wall experimental data for the evaporation of methanol into an air stream was modelled. A two dimensional axisymmetric model was used. The properties of the gas phase were assumed to be that of air at the experimental conditions (T=314 K, P =100,67 kPa). The boundary conditions are given in table 5. The mole fraction specified at wall 2 is equal to the equilibrium vapour phase concentration of methanol under the experimental conditions. At each velocity and for each mesh the distance of the first grid point away from the wall was calculated so that it would fall well within the viscous sub layer. The mesh was then refined until a converged answer was obtained. An entrance length equal to the length of the gas inlet section was used to allow for the flow to develop before reaching the wetted-wall section [13]. A decrease in cell size from the centre of the tube to the wall was used in order to decrease the total amount cells while still maintaining a fine grid near the wall. This was also done in the section between the inlet and the start of the wetted-wall section. From the centre to the wall the cell size was decreased in a quadratic fashion while a linear decrease was used from the inlet to the start of the wetted-wall section. Figure 10 shows details of the geometry.

Figure 11 compares the CFD and experimental results. This figure shows that the CFD model performs quite well in predicting the gas phase mass transfer coefficient. It must be noted that the experimental results plotted in this figure are for high flow rates of methanol where no wave formation was observed in the wetted-wall column. The assumption of a smooth surface in the wetted-wall section of the CFD model should therefore be reasonable. The velocity used in calculating the Reynolds number is that of the gas phase relative to the liquid surface [10]. Details of the mesh on which a converged answer was obtained are provided in table 6 for three different velocities. The answer was considered converged when the mass transfer coefficient did not change by more than 2% when a finer mesh was used.

Table 5 Boundary conditions: 2D axisymmetric wetted-wall model.

Boundary	Boundary condition
Inlet	*u* specified, default turbulence parameters, $x_A = 0.0$
Wall 1	$x_A = 0.0$, no-slip condition
Wall 2	$x_A = 0.314$, no-slip condition (wetted-wall)
Outlet	mass flow boundary

Table 6 Mesh detail for 2D axisymmetric wetted-wall model.

$Re_{G,r}$	Total number of elements	Distance of 1st node from wall [mm]	Number of nodes (see figure 10)		
			A	B	C
2929	9019	0.13	30	200	111
4393	18349	0.10	60	200	111
5858	30798	0.08	60	200	222

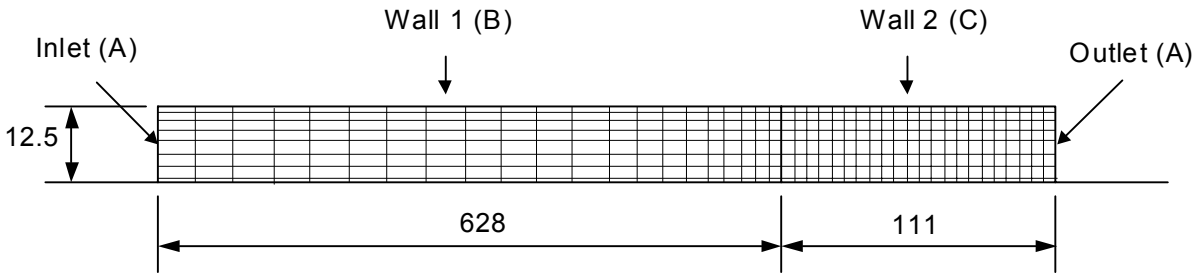

Figure 10 Geometry of wetted-wall column in 2D axisymmetric CFD model. Dimensions in (mm).

The approach used by previous researchers [7, 33] was followed in modelling the flow of the vapour phase in structured packing. Individual cross-corrugated junctions were modelled separately and the outlets used as inlets to the next junction. This process continued until 8 to 10 such junctions had been modelled. The properties of the chlorobenzene/ethylbenzene system was used to facilitate comparison between CFD and experimental distillation results and to compare the results with that of [7]. The dimensions of the packing junction is similar to that of Flexipac 350Y.

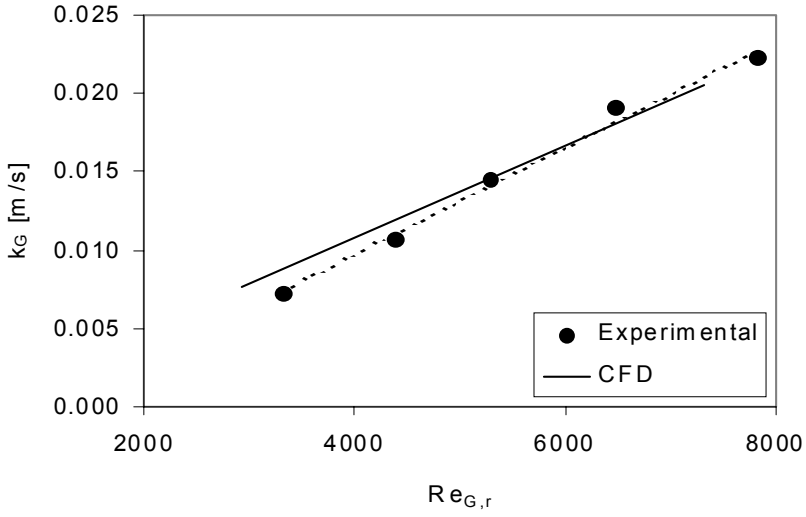

Figure 11 Comparison between CFD and wetted-wall experimental results for the evaporation of methanol into air. $Re_L(exp)=285$.

The geometry of a junction and the mesh detail are shown figure 12. The approach mentioned before in obtaining a converged grid was followed. A quadratic decrease in cell size from the centre of the junction to the wall was used to decrease the total amount of cells. An arbitrary mole fraction of 0.33 for the specie transferring from the wall was specified as a wall boundary condition. The boundary conditions are summarized in table 7. Figure 13 shows the CFD results for Re_G = 3705.

Table 7 Boundary conditions: Cross-corrugated packing junction

Boundary	Boundary condition
Inlets 1 & 2	*u, v, w* specified for first junction, default turbulence parameters, x_A = 0.0
Wall	x_A = 0.33, no-slip condition
Outlets 1 & 2	pressure boundary

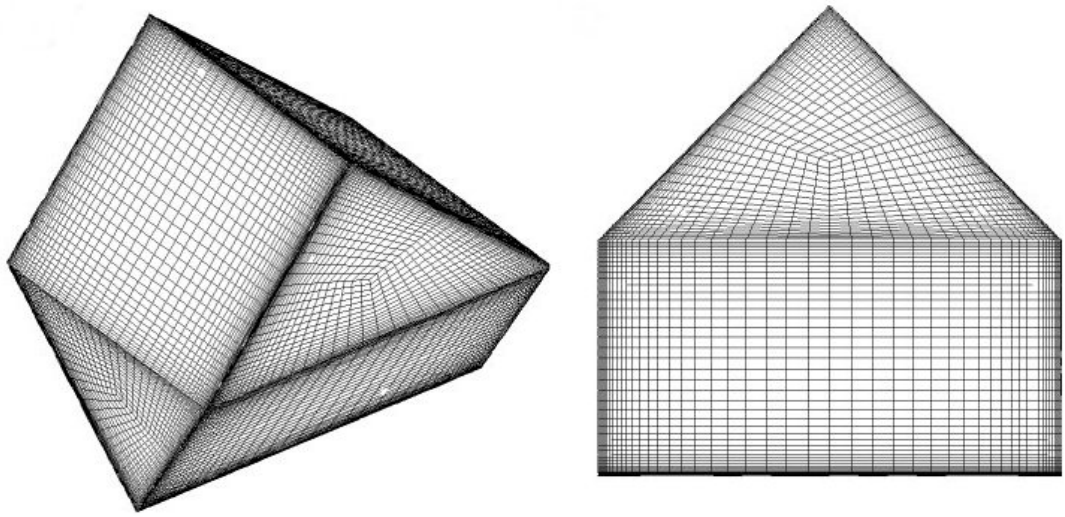

Figure 12 Packing junction and mesh detail (157500 elements). Distance of first node away from wall = 0.02 mm.

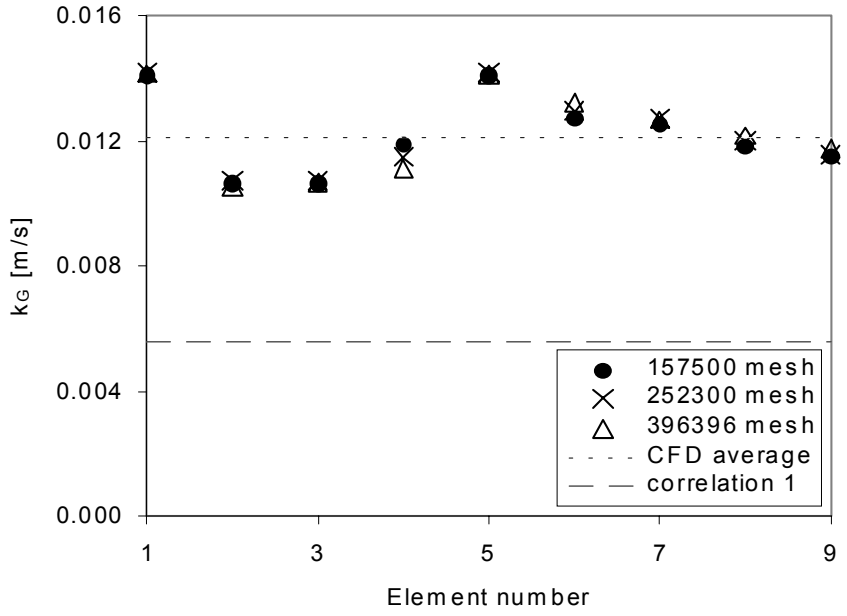

Figure 13 CFD results for Re_G = 3705.

The results for different meshes are shown for the first four junctions in this figure. It is evident that a converged solution was obtained with a mesh containing 157500 elements. The increase in the mass transfer rate from junction 3 to 5 is contributed to the secondary swirls that develop. This was also observed for heat transfer from the junction wall [7]. The mass transfer rate decreases towards a constant value after junction 5.

Also shown in figure 13 is the mass transfer coefficient calculated with correlation 1. The mass transfer coefficient predicted with this correlation is 50% smaller than the

CFD predicted value. This suggests that by using a correlation fitted on wetted-wall experimental data, the mass transfer rate would be severely under predicted in structured packing. This was indeed found to be the case with correlations 1 and 2 (see figures 2 to 6).

These results are preliminary and needs further investigation.

CONCLUSIONS

The wetted-wall mass transfer correlations developed in previous work were tested in the SRP and Delft structured packing models, using measured total reflux distillation data. By substituting the gas phase mass transfer correlations in the respective models with correlation 3 and 4, the accuracy of the models was improved. These correlations were fitted on wetted-wall experimental results for a liquid flowing over a packing surface. The SRP model gave the best results but there is some doubt as to the accuracy of the effective surface area calculated by this model. At conditions close to flooding the SRP model predicted an effective surface area of 78% compared to the 90% predicted by the Delft model. Both models tend predict higher values for pressure drop compared to experimental measurements. In general Flexipac 350Y performed better than predicted by these models. It is proposed that the gas phase mass transfer be measured and modelled separately by evaporating pure, organic liquids in a structured packing bed. Effective surface area measurements should also be made using organic liquids.

The use of computational fluid dynamics (CFD) as the basis for a gas phase mass transfer correlation was investigated. A low Reynolds number k-ε turbulence model was used. Since separated two-phase flow is a topic of ongoing research, only the gas phase was considered. The CFD model was first tested with wetted-wall experimental data for the evaporation of methanol. Satisfactory results were obtained. Only preliminary results with the structured packing model were discussed. The mass transfer coefficient predicted by the CFD model was 50% higher compared to a wetted-wall correlation.

ACKNOWLEDGEMENTS

Gratitude is expressed towards Koch for supplying the packing and allowing us to publish the distillation data. The financial support of the NRF (South Africa) is gratefully acknowledged.

NOMENCLATURE

a_e	effective surface area (m^2/m^3)
B	corrugation base length (m)
C	concentration ($mole/m^3$)
D_{AB}	binary diffusion coefficient (m^2/s)
d	diameter (m)
d_{eq}	equivalent diameter (m)

F_G	packing load factor, $F_G = u_{Gs}(\rho_G)^{0.5}$ (m/s.(kg/m^3)$^{0.5}$)
G	molar flow rate of vapour phase (mol/s)
h	corrugation crimp height (m)
$h_{packing}$	packing height (m)
HETP	height equivalent to a theoretical plate (m)
HTU	height of a transfer unit (m)
k	mass transfer coefficient (m/s)
L	molar flow rate of liquid phase (mol/s)
m	slope of equilibrium curve
N	molar flux (mol/s.m^2)
n	number of data points, number of stages
NTU	number of transfer units
p	perimeter (m)
S	corrugation side length (m)
u	velocity in x direction (m/s)
V	volumetric flow rate (m^3/s)
v	velocity in y direction (m/s)
w	velocity in z direction (m/s)
x	mole fraction

Dimensionless

Re_G	Gas phase Reynolds number, $Re_G = \rho_G u_G d_{eq}/\mu_G$
$Re_{G,r}$	Relative gas phase Reynolds number, $Re_G = \rho_G(u_G+u_{L,i})d_{eq}/\mu_G$
Re_L	Liquid phase Reynolds number, $Re_L = \rho_L V/(\mu_L p)$
Sc	Schmidt number, $Sc = \mu/(d_{eq}D_{AB})$
Sh	Sherwood number, $Sh = kd_{eq}/D_{AB}$

Greek symbols

δ	film thickness (m)
γ	stripping factor
μ	viscosity (Pa.s)
r	density (kg/m^3)

Subscript

A	specie A
B	specie B
b	bulk phase
G	gas phase
i	interface
L	liquid phase
m	mean
r	relative
s	superficial
T	total

REFERENCES

1. J.A. Rocha, *et al.* (1993), Ind. Eng. Chem. Res., 32, 641-651.
2. J.A. Rocha and J.L. Bravo (1996), Ind. Eng. Chem. Res., 35, 1660-1667.
3. Z. Olujic, *et al.* (1999), Chem. Eng. Process., 38, 683-695.
4. E. Brunazzi and A. Pagliante (1997), AIChE J., 43(2), 317-327.
5. E. Brunazzi and A. Paglianti (1997), Ind. Eng. Chem. Res., 36, 3792-3799.
6. I. Iliuta and F. Larachi (2001), Ind. Eng. Chem. Res., 40, 5140-5146.
7. J. Hodson (1997), Computational Fluid Dynamical Studies of Structured Distillation Packings, University of Aston, Birmingham, UK.
8. V.C. Patel, *et al.* (1985), AIAA J., 23(9), 1308-1319.
9. CFX-4.4 (1999), AEA Technology, Harwell, UK, Website: <http://www.software.aeat.com/cfx> [Accessed 22 February 2002].
10. A.B. Erasmus and I. Nieuwoudt (2001), Ind. Eng. Chem. Res., 40, 2310-2321.
11. E.R. Gilliland and T.K. Sherwood (1934), Ind. Eng. Chem., 26(5), 516-523.
12. R. Kafesjian, *et al.* (1961), AIChE J., 7(3), 463-466.
13. J.C. Crause and I. Nieuwoudt (1999), Ind. Eng. Chem. Res., 38, 4928-4932.
14. I. Nieuwoudt and J.C. Crause (1999), Ind. Eng. Chem. Res., 38, 4933-4937.
15. A. Dudukovic, *et al.* (1996), AIChE J., 42(1), 269-270.
16. L. Spiegel and W. Meier (1987), Inst. Chem. Eng. Symp. Ser., 104, A203-A215.
17. Z.A. Nawrocki, *et al.* (1991), Can. J. Chem. Eng., 69, 1336-1343.
18. J.R. Fair, *et al.* (2000), Ind. Eng. Chem. Res, 39, 1788-1796.
19. M.G. Shi and A. Mersmann (1985), Ger. Chem. Eng., 8, 87-96.
20. H.F. Johnstone and R.L. Pigford (1942), Trans. Am. Inst. Chem. Engrs., 38, 25.
21. J.L. Bravo, *et al.* (1985), Hydrocarbon Process., 64(1), 91-95.
22. J.D. Seader and E.J. Henley (1998), Separation Process Principles, John Wiley & Sons, New York.

23. A.S. Foust, *et al.* (1980), Principles of Unit Operations, 2nd ed, John Wiley & Sons, New York.

24. U. Onken and W. Arlt (1990), Recommended Test Mixtures for Distillation Columns, 2nd ed, The Institution of Chemical Engineers, Rugby, Warwickshire, England.

25. K. Stephan and H. Hildwein (1987), Recommended Data of Selected Compounds and Binary Mixtures, Chemistry Data Series, Vol. 4, Dechema, Frankfurt.

26. R.C. Reid, *et al.* (1986), The Properties of Gases and Liquids, 4th ed, McGraw-Hill, New York.

27. K. Onda, *et al.* (1968), J. Chem. Eng. Jpn., 1, 56.

28. H.-J. Verschoof, *et al.* (1999), Ind. Eng. Chem. Res., 38, 3663-3669.

29. T. Weimer and K. Schaber (1997), IChemE Symp. Ser., 142, 417-427.

30. D.L. Bennett and K.A. Ludwig (1994), Chem. Eng. Prog., 90(4), 72-79.

31. J.M. Van Baten, *et al.* (2001), Chem. Eng. Sci., 56, 813-821.

32. F.H. Yin, *et al.* (2000), Ind. Eng. Chem. Res., 39, 1369-1380.

33. M. Ciofalo, *et al.* (1996), Int. J. Heat Mass Transfer, 39(1), 165-192.

34. J. Stasiek, *et al.* (1996), Int. J. Heat Mass Transfer, 39(1), 149-164.

35. S. Nesic, *et al.* (1993), Can. J. Chem. Eng., 71(2), 28-34.

36. C. Rosén and C. Tragardh (1995), Chem. Eng. J., 59, 153-159.

37. J. Wang and S.A. Shirazi (2001), Int. J. Heat Mass Transfer, 44, 1817-1822.

38. G. Karimi and M. Kawaji (1998), Chem. Eng Sci., 53(20), 3501-3512.

39. G. Karimi and M. Kawaji (1999), Int. J. Multiphase Flow, 25, 1305-1319.

40. S. Peramanu and A. Sharma (1998), Can. J. Chem. Eng, 76(4), 211-223.

41. P. Bradshaw (1976), Turbulence, Springer-Verlag, Berlin.

42. M.B. Abbott and D.R. Basco (1989), Computational Fluid Dynamics. An Introduction for Engineers, Longman, Essex.

43. C.M. Rhie and W.L. Chow (1983), AIAA Journal, 21, 1525-1532.

44. J. Van Doormal and G.D. Raithby (1984), Numerical Heat Transfer, 7, 147-163.